Title:
Genomes of Poaceae sisters reveal key metabolic innovations preceding the evolution of grasses

Authors: Yuri Takeda-Kimura[1,2], Bethany Moore[1,†], Samuel Holden[3,‡], Sontosh K. Deb[4,§], Matt Barrett[5], David Lorence[6], Marcos V. V. de Oliveira[1], Jane Grimwood[7], Melissa Williams[7], Lori Beth Boston[7], Jerry Jenkins[7], Christopher Plott[7], Shengqiang Shu[8], Kerrie Barry[8], David M. Goodstein[8], Jeremy Schmutz[7,8], Matthew J. Moscou[3,9], Michael R. McKain[4], James H. Leebens-Mack[10*], Hiroshi A. Maeda[1*]

[1]Department of Botany, University of Wisconsin-Madison; Madison, WI, USA.
[2]Faculty of Agriculture, Yamagata University; Tsuruoka, Yamagata, Japan.
[3]The Sainsbury Laboratory, University of Cambridge; Norwich Research Park, Norwich, United Kingdom.
[4]Department of Biological Sciences, University of Alabama; Tuscaloosa, AL, USA.
[5]Australian Tropical Herbarium; Sir Robert Norman Building, James Cook University Cairns30 Campus, McGregor Road, Smithfield, Australia.
[6]National Tropical Botanical Garden; Kalaheo, Hawaii, USA.
[7]Genome Sequencing Center, HudsonAlpha Institute for Biotechnology; Huntsville, Alabama USA.
[8]US Department of Energy Joint Genome Institute; Berkeley, California USA.
[9]USDA-ARS, Cereal Disease Laboratory; St. Paul, MN, USA.
[10]Department of Plant Biology, University of Georgia; Athens, GA, USA.

Current addresses:
[†]Morgridge Institute for Research; Madison, WI, 53715, USA.
[‡]Faculty of Land and Food Systems, The University of British Columbia, Vancouver, BC, Canada.
[§]Department of Crop and Soil Sciences, North Carolina State University, Raleigh, NC 27695, USA

***Corresponding authors:**
James H. Leebens-Mack (jleebensmack@uga.edu), Hiroshi A. Maeda (maeda2@wisc.edu)

Abstract:

The grass family (Poaceae, Poales) holds immense economic and ecological significance, exhibiting unique metabolic traits, including dual starch and lignin biosynthetic pathways. To investigate when and how the metabolic innovations known in grasses evolved, we sequenced the genomes of four Poales species, including *Joinvillea ascendens* and *Ecdeiocolea monostachya* representing the sister clade to Poaceae. The *rho* whole genome duplication (ρWGD) in the ancestral lineage for all grasses contributed to the gene family expansions underlying cytosolic starch biosynthesis, whereas an earlier tandem duplication of *phenylalanine ammonia lyase* (*PAL*) gave rise to *phenylalanine/tyrosine ammonia lyase* (*PTAL*) responsible for the dual lignin biosynthesis. Integrated functional genomic and biochemical analyses of grass relatives further revealed the molecular basis of key metabolic innovations predating the evolution of grasses.

Key words:

metabolic innovations, gene duplication, genome multiplication, neofunctionalization, lignin, phenylalanine tyrosine ammonia lyase, Poales, Poaceae, Ecdeiocoleaceae, Joinvilleaceae

Joinvillea ascendens (Photo by David H. Lorence)

Introduction:

The grass family, Poaceae, emerged around 100 million years ago (Mya) within the monocot order Poales (*1*) and contains more than 11,000 species (**Fig. 1A**) (*1–3*). Grasses act as foundational primary producers for diverse ecosystems across the globe and contain many of the most economically important crops. Cereals, such as rice, wheat, and maize, provide more than 50% of calories for humans worldwide (*4*), while bioenergy crops, such as sugarcane and sorghum, produce abundant sugars and lignocellulosic biomass. Grasses exhibit a series of unique morphological and physiological traits, such as the highly specialized inflorescence, the ear, which has been a target for domestication to reduce shattering (*5–7*). Grasses also exhibit striking metabolic innovations, such as their ability to synthesize starch in both plastids and cytosol, leading to the starch-rich endosperm of grass seeds, e.g., grains and kernels (*8*). Grasses also have two entry pathways to synthesize lignin (**Fig. 1B**), the major cell wall phenolic polymer, which represents up to 30% of grass dry mass (*9*) and provides renewable aromatic feedstocks (*10–12*). Lignin is typically synthesized from the aromatic amino acid L-phenylalanine (Phe) via Phe ammonia-lyase (PAL) enzyme (**Fig. 1B**), but grasses can additionally utilize L-tyrosine (Tyr) to make lignin via the bifunctional Phe/Tyr ammonia-lyase (PTAL) (*13*, *14*). The PTAL pathway contributes to nearly half of grass lignin biosynthesis (*13*, *14*), potentially facilitating their rapid growth while depositing substantial lignin in their scattered vascular bundles (**Fig. 1B**). However, the evolutionary history and molecular basis of grass metabolic innovations are largely unknown.

Recent advancement in genome sequencing has permitted tracing whole genome duplications (WGD), gene family evolution, and gene innovations (*15–20*). Several key features of monocot genome evolutions include numerous polyploidy events (*21–23*), including the *rho* WGD (ρWGD) which occurred within the stem lineage leading to Poaceae (**Fig. 1A**) (*3*, *19*, *23*). The ρWGD event facilitated the evolution of complex traits and an increased speciation rate (*24*, *25*) in association with proliferation of MADS-box genes and diversification of the grass floral spikelet (*6*). The majority of sequenced Poales genomes are found in the Poaceae, especially cereal crops due to their agricultural significance (*26–29*). However, genome assemblies are currently unavailable from the sister clade to Poaceae, which includes two families, Ecdeiocoleaceae (N=3) and Joinvilleaceae (N=4) (*3*, *30*).

Here we document the utility of these sister genomes for comparative genomics and facilitate identification of genome and molecular features associated with grass-specific functional traits (**Fig. 1A**). Reference-quality genomes were first generated for *Joinvillea ascendens* Gaudich. ex Brongn. & Gris and *Ecdeiocolea monostachya* F.Muell., representing the sister clade to the entire grasses, along with *Pharus latifolius* L., a non-core Poaceae grass species, and the cattail species *Typha latifolia* L. representing the sister lineage to all other families in the order Poales (*3*, *30*, *31*). Our integrated genomic and biochemical analyses of grass relatives in the order Poales unveiled the evolutionary history and molecular basis of key metabolic innovations that predated the emergence of grasses. The study highlights the critical roles of both WGDs and tandem gene duplications underlying evolutionary innovations and identifies a gene editing target that can introduce the dual lignin entry pathway in non-grass plants. The Poales genomes obtained here offer valuable resources for dissecting diverse and complex grass traits uniquely evolved in this critical plant family.

Results:

Genomes of *Joinvillea ascendens*, *Ecdeiocolea monostachya*, *Pharus latifolius*, and *Typha latifolia* provide critical resources to study grass evolution

Ecdeiocolea monostachya is a wild perennial native to Western Australia and one of three species within the Ecdeiocoleaceae (**Fig. 1A**). The flow cytometry estimated between 38 to 42 chromosomes and haploid genome size of 980 Mb (4C of ~4.0 pg), consistent with an outcrossing species with an estimated chromosome number (2N) of 38 (*32*). The *E. monostachya* genome was assembled by HiFiAsm using PacBio HiFi long-reads, and gene models were predicted using *ab initio*, homology, and evidence-based gene models (see Methods). The final haploid consensus assembly of a heterozygous, diploid *E. monostachya* isolate EM_001 encompasses 897 Mb over 1,114 scaffolds with N50 of 1.7 Mb and a total of 27,801 genes, with 97.9% of the Embryophyte BUSCO genes (**Table 1**).

Joinvillea ascendens is native to the Hawaiian Islands and Oceania and one of four species within Joinvilleaceae (**Fig. 1A**). The genome of *J. ascendens* was sequenced to 125x coverage yielding a scaffold assembly with 18 chromosomes with a genome size of 1.21 Gb with N50 of 63.7 Mb and 29,122 protein coding genes, with 98% BUSCO score (**Table 1**). The *P. latifolius* genome was sequenced to a depth of 44x coverage yielding a chromosome level assembly spanning 1.12 Gb over 198 scaffolds. Gene models were inferred for 32,144 protein-coding genes, including 98.4% of the Embryophyte BUSCO genes (**Table 1**). As compared to the *P. latifolius* genome released by Ma et al. (*33*), the use of PacBio HiFi reads generated a reduced number of contigs (222 vs. 535) and slightly larger final genome size (1.12 Gb vs. 1.00 Gb). The *T. latifolia* genome was sequenced to depths of 74.70x coverage resulting in a chromosomal assembly including 215 Mb spanning the expected 15 chromosomes and one additional 54 Kb scaffold. A total of 22,107 protein-coding gene models were characterized in the *T. latifolia* genome including 99.7% of the Embryophyte BUSCO genes (**Table 1**). These three genomes were assembled using HiFiAsm, which integrates PacBio HiFi and Hi-C data, and polished using RACON (*34*). Scaffold orientation, ordering, and joining were based on Hi-C contact mapping, while evidence-based gene annotations were performed using Illumina RNAseq and PacBio IsoSeq reads (See Methods).

Variation in chromosomal structure across Poales genomes was elucidated using GENESPACE (*35*), which combines sequence similarity with gene order to robustly estimate orthology. Synteny patterns were consistent with the previously estimated timing of the ρWGD after divergence of Poaceae and its sister clade (**Fig. 1A**). A riverine plot reveals rearrangements of chromosomal blocks over the 120 My history of Poales (**Fig. 1C**). Gene family divergence and conservation were analyzed using 39 species with complete genomes, representing monocots with taxa focused in Poales along with representative eudicots, Magnoliids, and the basal angiosperms (ANA grade) (**table S1**). A Phylogenetic Phylogenetic Placement of Polyploidy Using Genomes (PUG) analysis (*3*, *30*, *31*) estimated a total of 2,493,258 putative paralog pairs from the 10,255 orthogroup trees across all taxa. After filtering for well supported nodes in the gene trees (see Methods), 21,105 putative paralog pairs provided support for unique duplication events (**Fig. 1D**). The comparisons between gene duplications on specific branches and previously characterized ancient polyploidy events showed that the highest number (3,200) of gene duplications was found on the branch leading to the last common ancestor of wheat (*Triticum aestivum*) and barley (*Hordeum vulgare*). The *rho* event—previously placed just prior to the diversification of core-grasses (*3*, *7*, *36*)—was supported with 3,004 gene duplications placed on the branch leading to the last common ancestor of all grasses (**Fig. 1D; table S2**). We also found 1122, 972, and 2196

146 gene duplications associated with the *sigma* WGD event (*37*), the *tau* WGD event (*3*, *38*), and the
147 maize allopolyploid event (*37*, *39*), respectively (**table S2**). Additionally, 868 and 936 unique gene
148 duplications were mapped to before the divergence of the BOP-PACMAD clades and the
149 PACMAD clade, respectively (**table S2**), likely representing either homoeologous exchange
150 between *rho* duplications (*40*) or possibly other types of duplication. Finally, we see evidence of
151 the *gamma* event (1,212 duplications) prior to the divergence of *Vitis* from other Pentapetalae (*41*,
152 *42*), as well as 803 unique duplications that map to branch leading to the common ancestor of all
153 eudicots (**table S2**). In sum, the genomes of *E. monostachya*, *J. ascendens*, *P. latifolius,* and *T.*
154 *latifolia* enable improved resolution of genome evolution with the grasses and prior to their origin.

155 **Duplication of genes involved in starch and fatty acid biosynthesis during grass evolution**

156 Starch stores carbon and energy for maintaining metabolism and growth (*43*, *44*). Grasses have
157 starch-rich seeds that support rapid seedling establishment (*45*) and provide the major source of
158 calories consumed by humans (e.g., cereal grains and kernels). Besides plastids where starch is
159 stored and typically made (*46*), grass endosperms can synthesize starch also in the cytosol (*8*, *47*)
160 (**Fig. 2A**). To investigate the origin of the cytosolic starch biosynthesis, we constructed
161 phylogenetic trees of three genes required for the cytosolic starch biosynthesis—ADP-glucose
162 pyrophosphorylase (AGPase) large and small subunits (LSU and SSU, respectively) and ADP
163 glucose transporter (**Fig. 2A**). Grasses have four types of AGPase LSUs with the duplication of
164 Type 3 AGPase LSUs that likely generated Type 2 cytosolic AGPase LSUs (*8*). Consistent with
165 this notion, our phylogeny showed two distinct, well-supported Type 3 and Type 2 AGPase LSU
166 clades both having sequences from *P. latifolius* and another non-core grass, *Streptochaeta*
167 *angustifolia* (*7*). In contrast, *J. ascendens* and *E. monostachya* sequences were found in their
168 outgroup (**Fig. 2B; fig. S1A**), suggesting that the duplication event occurred within grasses.
169 Similarly, AGPase SSUs duplicated within grasses, giving rise to Type 1 AGPase SSUs (**Fig. 2C;**
170 **fig. S1B**), which is dual localized but reside in the cytosol in the endosperm, unlike Type 2 AGPase
171 SSUs targeted to the plastids in leaves (*48*). The plastidial ADP glucose transporter, required to
172 import ADP-glucose into the plastids (**Fig. 2A**) (*8*), also underwent gene duplication within the
173 common ancestor of all grasses (**Fig. 2D**), giving rise to the plastidial ADP glucose transporter
174 within the Type 2 Plastidial Adenine Nucleotide Transporters (PANTs) (*49*). The long branch
175 leading to the grass-specific plastidial ADP glucose transporter suggests potential positive
176 selection for neofunctionalization. Notably, however, *J. ascendens* and all grasses, including *S.*
177 *angustifolia* and *P. latifolius*, had both Type 1 and Type 2 PANTs (**Fig. 2D**). This finding suggests
178 that there was an earlier duplication event preceding the emergence of grasses, giving rise to the
179 Type 2 PANTs, from which the plastidial ADP glucose transporter later evolved.
180 Grasses also have a unique biochemical feature for fatty acid biosynthesis. Plants typically
181 have heteromeric prokaryotic-type and homomeric eukaryotic-type acetyl-CoA carboxylase
182 (ACCase) in the cytosol and plastids, respectively, whereas grasses have homomeric eukaryotic-
183 type ACCase in both cytosol and plastids (*50*, *51*) (**Fig. 2A**). This makes grasses sensitive to certain
184 herbicides that inhibit homomeric but not heteromeric ACCase (*50*, *52*). Notably, the homomeric
185 eukaryotic-type *ACCase* gene duplicated in ancestral non-grass graminids, giving rise to the
186 plastidic homomeric eukaryotic-type ACCase in grasses as well as *J. ascendens* and *E.*
187 *monostachya* (**Fig. 2E**). These results together revealed the evolutionary history of metabolic
188 genes underlying the unique metabolic traits of grasses, some of which have already appeared
189 *before* the emergence of grasses and ρWGD.

PTAL evolved within a common ancestor of grasses and non-grass graminid *Joinvillea*, before ρWGD and the appearance of grasses.

Utilizing these novel genomic resources, we further investigated the evolutionary history of the dual lignin entry pathways, uniquely found in grasses (**Fig. 1B**) (*13*, *14*, *53*). Synteny analyses revealed that *J. ascendens* has two copies of *PAL/PTAL* homologs (Joasc.05G060400.1, Joasc.05G060500.1) located in tandem within the same syntenic block at the chromosome 5 (**Fig. 3A**), whereas the corresponding syntenic block in *Ananas comosus* (pineapple) has just one *PAL/PTAL* homolog. Within grasses, the *PAL/PTAL* syntenic block was further duplicated in association with the ρWGD, and *PAL* genes in one of the two duplicated blocks were expanded in core grasses (**Fig. 3A**). One *PAL/PTAL* copy within these syntenic blocks in grasses encodes previously characterized or predicted PTAL enzymes (*14*). Analyses of *Ks* values (synonymous substitutions) for genes within and between *PAL/PTAL* syntenic blocks further supports the timing of the ancestral *PAL/PTAL* tandem duplication before ρWGD **(fig. S2)** and the origin of Poaceae.

In contrast to the findings of the synteny analysis, the Maximum Likelihood (ML) gene tree for the *PAL/PTAL* gene family resolved *PAL* homologs from *J. ascendens*, and *E. monostachya* on a grade leading to a clade with all *PTAL* homologs from *J. ascendens*, *E. monostachya* and grasses (**figs. S3 and S4**). Using the TreeSolve dynamic programming algorithm for species-tree-aware estimation of the *PAL/PTAL* tree while accounting for the gene duplication-and-loss process (*54*), monophyly of the *PAL* and *PTAL* orthologs was recovered with a support values of 100% for each clade **(Fig. 3B, fig. S5)**. Consistent with the inference of an ancestral tandem duplication based on the synteny analysis (**Fig. 3A**), *J. ascendens* Joasc.05G060500.1 and *E. monostachya* Emoptg000374l_1G000600.1 genes formed a clade sister to a clade with all grass *PAL* orthologs, and Joasc.05G060400.1 and Emoptg000374l_1G000630.1 were in a clade sister to all grass *PTAL* genes (**Fig. 3B, fig. S5**). In sum, these analyses implicate divergence of *PAL* and *PTAL* and neofunctionalization of *PTAL* following a tandem duplication in a graminid ancestor of the grasses.

The His140 residue, located at the substrate binding pocket, was previously shown to be critical for the Tyr substrate recognition in the bacterial TAL enzyme (*55*). We noted that the corresponding His140 residues were present in PTAL orthologs of all grasses, including both of the *S. angustifolia* enzymes (strangu_020769−RA and strangu_019386−RA), as well as one of each enzyme from *J. ascenden*s (Joasc.05G060400.1) and *E. monostachya* (Emoptg000374l_1G000630.1), suggesting that these proteins may be functional PTAL enzymes. To test this hypothesis experimentally, we cloned, expressed, and purified the recombinant enzymes of PAL/PTAL orthologs from *S. angustifolia*, *J. ascendens*, and *E. monostachya*, along with PALs and PTALs from *Sorghum bicolor* (SbPAL and SbPTAL) and *Brachypodium distachyon* (BdPAL and BdPTAL) as positive controls (*14*, *56*). All of these purified enzymes showed robust PAL activity, efficiently converting Phe to cinnamic acid (CA) as confirmed by HPLC analysis (**Fig. 3C**), unlike negative controls (i.e., boiled enzyme or no substrate controls, **fig. S6**). Efficient TAL activity, the production of *p*CA from Tyr, was observed from SbPTAL, BdPTAL, strangu_020769−RA, strangu_019386−RA, Emoptg000374l_1G000630.1, and Joasc.05G060400.1, whereas much lower TAL activity was detected from the remaining enzymes (**Fig. 3C**). These results showed that the PAL/PTAL orthologs with His140 are bifunctional PTAL enzymes having both PAL and TAL activity. Therefore, we named both of *S. angustifolia* enzymes and one of *E. monostachya*, and *J. ascendens* enzymes having His140 as SaPTAL-a, SaPTAL-b, EmoPTAL, and JaPTAL, whereas another one of *E. monostachya*, and *J. ascendens* enzymes with Phe140 as EmoPAL and JaPAL, respectively (**Fig. 3B**).

Enzyme kinetic analyses further revealed that the apparent K_m of these PTAL enzymes for

236 Tyr were 11 to 19 μM, whereas those of PAL enzymes were much higher (3449-6211 μM) and
237 hence inefficient in utilizing Tyr. The k_{cat} values of the TAL activity were approximately twice
238 higher for PTALs than for PALs (**Fig. 3, D and E**; **table S2**). Consequently, the catalytic efficiency
239 (k_{cat}/K_m) of TAL activity for PTAL enzymes were much higher (485-fold in average) than those
240 for PAL enzymes (**Fig. 3, D and E; table S3**). These quantitative data further support that *S.*
241 *angustifolia*, *E. monostachya*, and *J. ascendens* have at least one PTAL enzyme having strong
242 TAL activity. We also noted that grass PTAL enzymes showed higher K_m toward Phe (150-227
243 μM) than graminid PTALs (64-66 μM) (**table S3**), leading to ~3.1-fold higher TAL/PAL activity
244 ratio for PTALs from grasses than non-grass graminids (**fig. S7A**). These experimental data
245 demonstrate that the bifunctional PTAL enzymes emerged within the common ancestor of grasses
246 and non-grass graminids (e.g., *J. ascendens*), and later gained higher TAL/PAL ratio in grasses.

247 **Ile112 and His140 are critical for acquisition of the TAL activity in graminid PTALs.**

248 To experimentally test the role of His140 for the acquisition of TAL activity, site-directed
249 mutagenesis was conducted on the PAL and PTAL enzymes of grasses and non-grass graminids
250 characterized above. The conversion of Phe140 to His in PAL enzymes (e.g., $JaPAL^{F140H}$)
251 increased overall TAL activity (9.7-fold in k_{cat}/K_m average) with significant reduction of K_m values
252 towards Tyr (**table S3**). The reciprocal mutants of PTAL enzymes (e.g., $JaPTAL^{H125F}$) also
253 exhibited decreased TAL activity (0.01-fold k_{cat}/K_m in average) with significant increase in K_m
254 towards Tyr (**fig. S7B; table S3**). These results support the importance of His140 for TAL activity,
255 consistent with prior studies (*55*, *57*); however, the introduction of His140 itself was not *sufficient*
256 to convert PALs into PTALs. The catalytic efficiency of TAL activity (k_{cat}/K_m) of PAL^{F140H}
257 mutants was still much lower (~10% in average) than that of wild-type PTALs, because of the
258 much higher K_m values (222-450 μM) than wild-type PTALs (11-19 μM) (**fig, S7B; table S3**).
259 Furthermore, $PTAL^{H140F}$ mutants still showed higher TAL activity than that of wild-type PALs
260 (e.g., K_m value of 531-765 vs. 3448-6211 μM). Thus, unlike the bacterial TAL enzyme (*57*), other
261 residues besides the His140 are required for the acquisition of strong TAL activity in PTALs of
262 grasses and closely-related non-grass graminids.

263 To search for the additional residue(s) required for the efficient TAL activity, we first
264 conducted a positive selection analysis of *dN/dS* (nonsynonymous to synonymous substitution
265 rate) using PAML (*58*). A total of 30 positively selected sites were identified between the PTAL
266 vs. PAL clade of the graminids with a probability of >0.7 (**table S4**). A phylogeny-guided amino
267 acid sequence comparison (*59*) utilizing the phylogenetic distribution of the functional PAL and
268 PTALs (**Fig. 3**) identified 16 residues, besides His140, that are highly conserved in PTAL enzymes
269 (**Fig. 4A; fig. S8**), all of which were under positive selection (**table S4**). Eight residues (magenta
270 in **Fig. 4A**) were highly conserved within PAL and PTAL groups but distinct between these two
271 groups; the additional 8 residues (purple in **Fig. 4A**) were highly conserved only among PTALs
272 and variable in different PALs (**Fig 4A; table S4**). Based on a homology model of JaPAL
273 generated using the well-characterized parsley PAL structure as a template (PDB:6F6T) (*60*), most
274 of these 16 residues were found to be located near the active site, except for a few peripheral
275 residues highlighted in purple (**Fig. 4B**).

276 To test functions of these residues, $JaPAL^{F140H}$ was further mutated at these 8 magenta
277 residues or both magenta and purple (total 16) residues from PAL- to PTAL-type (**table S4**),
278 generating $JaPAL^{F140H_MUT8}$ and $JaPAL^{F140H_MUT16}$, respectively. The apparent K_m value of
279 $JaPAL^{F140H_MUT8}$ (17.9 μM) became significantly improved than that of the $JaPAL^{F140H}$ single
280 mutant (222.7 μM) and approached closely to that of wild-type JaPTAL (10.9 μM) with the similar

281 k_{cat} (**Fig. 4C; table S3**). The JaPAL^{F140H_MUT16} mutant also showed significantly improved K_m
282 (42.2 μM) for TAL activity than JaPAL^{F140H} (and JaPAL wild-type) but to a lesser extent than
283 JaPAL^{F140H_MUT8} (17.9 μM, **Fig. 4C**). Thus, these results demonstrate that some of these 8 magenta
284 residues, besides His140, are involved in the efficient TAL activity of non-grass graminid PTALs.
285 To determine which of the eight magenta residues are essential in the conversion of PAL to
286 PTAL enzyme, each one of these residues on JaPAL^{F140H_MUT8} was mutated back to the PAL type,
287 one by one. The substitution of seven out of eight residues had no to minor impacts on the overall
288 TAL activity (**Fig. 4D**). In contrast, when the I112S substitution was introduced to
289 JaPAL^{F140H_MUT8} to make JaPAL^{F140H_MUT8_I112S}, TAL activity was significantly decreased because
290 of the drastic increase of K_m and slight reduction of k_{cat} (**Fig. 4D; table S3**). Based on the structure
291 models of JaPAL and JaPTAL proteins generated with parsley PAL and sorghum PTAL structures
292 (*56*, *61*), respectively, as a template (**Fig. 4E**), the Ser/Ile112 is not in direct contact with the
293 substrate but is located next to the Tyr113/98 (for PAL/PTAL), a critical proton acceptor for the
294 catalysis. Therefore, the Ile112 residue of the PTAL enzyme near the active site appears to be
295 crucial for the efficient TAL activity.

296 **F140H and S112I substitutions are sufficient to change plant PALs into bifunctional PTALs.**

297 To further test the role of the Ile112 residue, the reciprocal S112I mutation was introduced to the
298 JaPAL wild-type and JaPAL^{F140H} single mutant to generate the JaPAL^{S112I} single and
299 JaPAL^{F140H_S112I} double mutants, respectively. While k_{cat} was not drastically affected by these
300 mutations, K_m of JaPAL^{F140H_S112I} for Tyr (17.5 μM) became significantly lower than those of the
301 wild-type JaPAL (4859 μM) and the single mutants JaPAL^{F140H} and JaPAL^{S112I} (223 μM and 354
302 μM, respectively) and reached to the level of wild-type JaPTAL (11.0 μM) (**Fig. 4F**). Therefore,
303 Ile112 is essential for gaining the efficient TAL activity. Strikingly, introduction of these two
304 amino acid substitutions equivalent to F140H and S112I in a distantly-related PAL from
305 *Arabidopsis thaliana* (*55*, *62*) (AtPAL1^{F144H_S116I}) also conferred efficient TAL activity. The
306 AtPAL1^{F144H_S116I} mutant showed dramatic reduction in its K_m towards Tyr (20.2 μM) as compared
307 to wild-type AtPAL1 (3070 μM) and its single mutants, AtPAL1^{F144H} and AtPAL1^{S116I} (314 μM
308 and 515 μM, respectively). Overall, the kinetic behavior of the AtPAL1^{F144H_S116I} and
309 JaPAL^{H140F_I112S} double mutants were similar (**Fig. 4, F and G; table S3**). Thus, the introduction
310 of two key residues Ile112 and His140, identified from the PTAL evolutionary analysis in Poales,
311 can alter monofunctional PALs into bifunctional PTALs even in a distantly-related plant PAL
312 enzyme.
313

Discussion:

Genomes of closely related species in sister lineages provide critical resources to dissect the genetic and molecular basis of unique traits that evolved in a target organism(s). For example, the chimpanzee and bonobo genomes have accelerated our understanding of the evolution of human traits (*63*, *64*). In the current study, integrated genomic and biochemical analyses of Poales that are close-relative to core-grasses unveiled the evolutionary origin and molecular basis of key metabolic innovations that predated the emergence of grasses. While some genes involved in the cytosolic starch biosynthetic pathway emerged through the ρWGD, a preceding duplication into PANT Type 1 and 2 potentiated the evolution of ADP-glucose transport across the plastid membrane (**Fig. 2E**). Strikingly, the dual lignin entry pathway catalyzed by bifunctional PTAL enzyme, which was believed to be specific to grasses (*14*), actually emerged *before* the evolution of grasses at the common ancestor of Joinvilleaceae, Ecdeiocoleaceae, and Poaceae. Although WGD-associate diversification has been attributed to sub/neofunctionalization of duplicates leading to morphological and functional innovations (*65*, *66*), our results uncovered that tandemly duplicated gene families also contribute to evolutionary innovations, through subsequent neofunctionalization and further expansion by later WGD (**Fig. 3**).

Precise determination of the timing of the PTAL evolution also revealed its underlying molecular basis. A novel residue Ile112 responsible for the transition from PAL to PTAL function is located at the 'inner mobile loop' (**Fig. 4E**). Based on prior structure analyses (*61*, *67*), such modification likely alters the substrate binding pocket and improves TAL activity. We further demonstrated that simultaneously introducing two substitutions, Ser112 to Ile and Phe140 to His, converted both monocot and dicot PAL into PTAL enzymes (**Fig. 4, F and G**). The dual entry pathway via PTAL likely enabled efficient synthesis of phenylpropanoids in fast-growing grasses that still accumulate lignin at up to 30% of dry weight (*9*, *12*, *68*). Therefore, leveraging insights from grass evolution, the introduction of a second entry pathway of lignin biosynthesis, via the Ile112 and His140 residues, presents a promising gene editing strategy to enhance the production of diverse phenylpropanoid compounds in various plants.

Grasses have many derived functional traits that are hypothesized to have contributed to their evolutionary success of this prominent plant family with immense economic and ecological significance (*45*, *69*). While many grass genomes have been sequenced (*26–29*), the ancestral characteristics of grasses remain poorly understood due to the lack of reference-quality genomes in the sister lineage to the grass family. The novel Poales genomes obtained in this study now offer valuable resources to dissect complex traits uniquely evolved in grasses and their relatives. Understanding the evolutionary basis of grass-specific traits will inform efforts to conserve grass-dominated ecosystems and accelerate grass breeding and engineering for sustainable production of food, feed, bioenergy, and biomaterials.

References:

1. W. Huang, L. Zhang, J. T. Columbus, Y. Hu, Y. Zhao, L. Tang, Z. Guo, W. Chen, M. McKain, M. Bartlett, C.-H. Huang, D.-Z. Li, S. Ge, H. Ma, A well-supported nuclear phylogeny of Poaceae and implications for the evolution of C4 photosynthesis. *Mol. Plant* **15**, 755–777 (2022).
2. T. J. Givnish, M. Ames, J. R. McNeal, M. R. McKain, P. R. Steele, C. W. Depamphilis, S. W. Graham, J. C. Pires, D. W. Stevenson, W. B. Zomlefer, Others, Assembling the tree of the monocotyledons: plastome sequence phylogeny and evolution of Poales1. *Ann. Mo. Bot. Gard.* **97**, 584–616 (2010).
3. M. R. McKain, H. Tang, J. R. McNeal, S. Ayyampalayam, J. I. Davis, C. W. dePamphilis, T. J. Givnish, J. C. Pires, D. W. Stevenson, J. H. Leebens-Mack, A Phylogenomic Assessment of Ancient Polyploidy and Genome Evolution across the Poales. *Genome Biol. Evol.* **8**, 1150–1164 (2016).
4. ESS: 9.3 World Calories - Total. https://www.fao.org/economic/the-statistics-division-ess/chartroom-and-factoids/chartroom/93-world-calories-total/en/.
5. Z. Lin, X. Li, L. M. Shannon, C.-T. Yeh, M. L. Wang, G. Bai, Z. Peng, J. Li, H. N. Trick, T. E. Clemente, J. Doebley, P. S. Schnable, M. R. Tuinstra, T. T. Tesso, F. White, J. Yu, Parallel domestication of the Shattering1 genes in cereals. *Nat. Genet.* **44**, 720–724 (2012).
6. Y. Wang, X. Bi, J. Zhong, Revisiting the origin and identity specification of the spikelet: A structural innovation in grasses (Poaceae). *Plant Physiol.* **190**, 60–71 (2022).
7. A. S. Seetharam, Y. Yu, S. Bélanger, L. G. Clark, B. C. Meyers, E. A. Kellogg, M. B. Hufford, The Genome and the Evolution of the Grasses. *Front. Plant Sci.* **12**, 710383 (2021).
8. S. Comparot-Moss, K. Denyer, The evolution of the starch biosynthetic pathway in cereals and other grasses. *J. Exp. Bot.* **60**, 2481–2492 (2009).
9. R. Bhatia, J. A. Gallagher, L. D. Gomez, M. Bosch, Genetic engineering of grass cell wall polysaccharides for biorefining. *Plant Biotechnol. J.* **15**, 1071–1092 (2017).
10. A. J. Ragauskas, G. T. Beckham, M. J. Biddy, R. Chandra, F. Chen, M. F. Davis, B. H. Davison, R. A. Dixon, P. Gilna, M. Keller, P. Langan, A. K. Naskar, J. N. Saddler, T. J. Tschaplinski, G. A. Tuskan, C. E. Wyman, Lignin Valorization: Improving Lignin Processing in the Biorefinery. *Science* **344**, 1246843–1246843 (2014).
11. R. Rinaldi, R. Jastrzebski, M. T. Clough, J. Ralph, M. Kennema, P. C. A. Bruijnincx, B. M. Weckhuysen, Paving the Way for Lignin Valorisation: Recent Advances in Bioengineering, Biorefining and Catalysis. *Angew. Chem. Int. Ed.* **55**, 8164–8215 (2016).
12. T. Umezawa, Lignin modification *in planta* for valorization. *Phytochem. Rev.*, 1–23 (2018).
13. J. Rosler, F. Krekel, N. Amrhein, J. Schmid, Maize phenylalanine ammonia-lyase has tyrosine ammonia-lyase activity. *Plant Physiol.* **113**, 175–179 (1997).
14. J. Barros, J. C. Serrani-Yarce, F. Chen, D. Baxter, B. J. Venables, R. A. Dixon, Role of bifunctional ammonia-lyase in grass cell wall biosynthesis. *Nat. Plants* **2**, 16050 (2016).
15. Y. Van de Peer, T.-L. Ashman, P. S. Soltis, D. E. Soltis, Polyploidy: an evolutionary and ecological force in stressful times. *Plant Cell* **33**, 11–26 (2021).
16. F. Almeida-Silva, Y. Van de Peer, Whole-genome Duplications and the Long-term Evolution of Gene Regulatory Networks in Angiosperms. *Mol. Biol. Evol.* **40** (2023).
17. N. Walden, D. A. German, E. M. Wolf, M. Kiefer, P. Rigault, X.-C. Huang, C. Kiefer, R. Schmickl, A. Franzke, B. Neuffer, K. Mummenhoff, M. A. Koch, Nested whole-genome duplications coincide with diversification and high morphological disparity in Brassicaceae. *Nat. Commun.* **11**, 3795 (2020).
18. K. C. Moharana, T. M. Venancio, Polyploidization events shaped the transcription factor repertoires in legumes (Fabaceae). *Plant J.* **103**, 726–741 (2020).

395 19. T. Zhang, W. Huang, L. Zhang, D.-Z. Li, J. Qi, H. Ma, Phylogenomic profiles of whole-genome
396 duplications in Poaceae and landscape of differential duplicate retention and losses among major
397 Poaceae lineages. *Nat. Commun.* **15**, 3305 (2024).

398 20. J. W. Clark, P. C. J. Donoghue, Whole-Genome Duplication and Plant Macroevolution. *Trends Plant*
399 *Sci.* **23**, 933–945 (2018).

400 21. A. H. Paterson, J. E. Bowers, B. A. Chapman, Ancient polyploidization predating divergence of the
401 cereals, and its consequences for comparative genomics. *Proc. Nat. Acad. Sci. U. S. A.* **101**, 9903–
402 9908 (2004).

403 22. J. Yu, J. Wang, W. Lin, S. Li, H. Li, J. Zhou, P. Ni, W. Dong, S. Hu, C. Zeng, J. Zhang, Y. Zhang, R.
404 Li, Z. Xu, S. Li, X. Li, H. Zheng, L. Cong, L. Lin, J. Yin, J. Geng, G. Li, J. Shi, J. Liu, H. Lv, J. Li, J.
405 Wang, Y. Deng, L. Ran, X. Shi, X. Wang, Q. Wu, C. Li, X. Ren, J. Wang, X. Wang, D. Li, D. Liu, X.
406 Zhang, Z. Ji, W. Zhao, Y. Sun, Z. Zhang, J. Bao, Y. Han, L. Dong, J. Ji, P. Chen, S. Wu, J. Liu, Y.
407 Xiao, D. Bu, J. Tan, L. Yang, C. Ye, J. Zhang, J. Xu, Y. Zhou, Y. Yu, B. Zhang, S. Zhuang, H. Wei,
408 B. Liu, M. Lei, H. Yu, Y. Li, H. Xu, S. Wei, X. He, L. Fang, Z. Zhang, Y. Zhang, X. Huang, Z. Su,
409 W. Tong, J. Li, Z. Tong, S. Li, J. Ye, L. Wang, L. Fang, T. Lei, C. Chen, H. Chen, Z. Xu, H. Li, H.
410 Huang, F. Zhang, H. Xu, N. Li, C. Zhao, S. Li, L. Dong, Y. Huang, L. Li, Y. Xi, Q. Qi, W. Li, B.
411 Zhang, W. Hu, Y. Zhang, X. Tian, Y. Jiao, X. Liang, J. Jin, L. Gao, W. Zheng, B. Hao, S. Liu, W.
412 Wang, L. Yuan, M. Cao, J. McDermott, R. Samudrala, J. Wang, G. K.-S. Wong, H. Yang, The
413 Genomes of Oryza sativa: A History of Duplications. *PLOS Biology* **3**, e38 (2005).

414 23. H. Tang, J. E. Bowers, X. Wang, A. H. Paterson, Angiosperm genome comparisons reveal early
415 polyploidy in the monocot lineage. *Proc. Natl. Acad. Sci. U. S. A.* **107**, 472–477 (2010).

416 24. S. Ohno, Evolution by Gene Duplication. 1970, London: G. *Allen Google Scholar*.

417 25. K. Vanneste, G. Baele, S. Maere, Y. Van de Peer, Analysis of 41 plant genomes supports a wave of
418 successful genome duplications in association with the Cretaceous-Paleogene boundary. *Genome Res.*
419 **24**, 1334–1347 (2014).

420 26. S. A. Goff, D. Ricke, T.-H. Lan, G. Presting, R. Wang, M. Dunn, J. Glazebrook, A. Sessions, P. Oeller,
421 H. Varma, D. Hadley, D. Hutchison, C. Martin, F. Katagiri, B. M. Lange, T. Moughamer, Y. Xia, P.
422 Budworth, J. Zhong, T. Miguel, U. Paszkowski, S. Zhang, M. Colbert, W.-L. Sun, L. Chen, B. Cooper,
423 S. Park, T. C. Wood, L. Mao, P. Quail, R. Wing, R. Dean, Y. Yu, A. Zharkikh, R. Shen, S.
424 Sahasrabudhe, A. Thomas, R. Cannings, A. Gutin, D. Pruss, J. Reid, S. Tavtigian, J. Mitchell, G.
425 Eldredge, T. Scholl, R. M. Miller, S. Bhatnagar, N. Adey, T. Rubano, N. Tusneem, R. Robinson, J.
426 Feldhaus, T. Macalma, A. Oliphant, S. Briggs, A draft sequence of the rice genome (Oryza sativa L.
427 ssp. japonica). *Science* **296**, 92–100 (2002).

428 27. J. Yu, S. Hu, J. Wang, G. K.-S. Wong, S. Li, B. Liu, Y. Deng, L. Dai, Y. Zhou, X. Zhang, M. Cao, J.
429 Liu, J. Sun, J. Tang, Y. Chen, X. Huang, W. Lin, C. Ye, W. Tong, L. Cong, J. Geng, Y. Han, L. Li,
430 W. Li, G. Hu, X. Huang, W. Li, J. Li, Z. Liu, L. Li, J. Liu, Q. Qi, J. Liu, L. Li, T. Li, X. Wang, H. Lu,
431 T. Wu, M. Zhu, P. Ni, H. Han, W. Dong, X. Ren, X. Feng, P. Cui, X. Li, H. Wang, X. Xu, W. Zhai,
432 Z. Xu, J. Zhang, S. He, J. Zhang, J. Xu, K. Zhang, X. Zheng, J. Dong, W. Zeng, L. Tao, J. Ye, J. Tan,
433 X. Ren, X. Chen, J. He, D. Liu, W. Tian, C. Tian, H. Xia, Q. Bao, G. Li, H. Gao, T. Cao, J. Wang, W.
434 Zhao, P. Li, W. Chen, X. Wang, Y. Zhang, J. Hu, J. Wang, S. Liu, J. Yang, G. Zhang, Y. Xiong, Z.
435 Li, L. Mao, C. Zhou, Z. Zhu, R. Chen, B. Hao, W. Zheng, S. Chen, W. Guo, G. Li, S. Liu, M. Tao, J.
436 Wang, L. Zhu, L. Yuan, H. Yang, A draft sequence of the rice genome (Oryza sativa L. ssp. indica).
437 *Science* **296**, 79–92 (2002).

438 28. P. S. Schnable, D. Ware, R. S. Fulton, J. C. Stein, F. Wei, S. Pasternak, C. Liang, J. Zhang, L. Fulton,
439 T. A. Graves, P. Minx, A. D. Reily, L. Courtney, S. S. Kruchowski, C. Tomlinson, C. Strong, K.
440 Delehaunty, C. Fronick, B. Courtney, S. M. Rock, E. Belter, F. Du, K. Kim, R. M. Abbott, M. Cotton,
441 A. Levy, P. Marchetto, K. Ochoa, S. M. Jackson, B. Gillam, W. Chen, L. Yan, J. Higginbotham, M.

Cardenas, J. Waligorski, E. Applebaum, L. Phelps, J. Falcone, K. Kanchi, T. Thane, A. Scimone, N. Thane, J. Henke, T. Wang, J. Ruppert, N. Shah, K. Rotter, J. Hodges, E. Ingenthron, M. Cordes, S. Kohlberg, J. Sgro, B. Delgado, K. Mead, A. Chinwalla, S. Leonard, K. Crouse, K. Collura, D. Kudrna, J. Currie, R. He, A. Angelova, S. Rajasekar, T. Mueller, R. Lomeli, G. Scara, A. Ko, K. Delaney, M. Wissotski, G. Lopez, D. Campos, M. Braidotti, E. Ashley, W. Golser, H. Kim, S. Lee, J. Lin, Z. Dujmic, W. Kim, J. Talag, A. Zuccolo, C. Fan, A. Sebastian, M. Kramer, L. Spiegel, L. Nascimento, T. Zutavern, B. Miller, C. Ambroise, S. Muller, W. Spooner, A. Narechania, L. Ren, S. Wei, S. Kumari, B. Faga, M. J. Levy, L. McMahan, P. Van Buren, M. W. Vaughn, K. Ying, C.-T. Yeh, S. J. Emrich, Y. Jia, A. Kalyanaraman, A.-P. Hsia, W. B. Barbazuk, R. S. Baucom, T. P. Brutnell, N. C. Carpita, C. Chaparro, J.-M. Chia, J.-M. Deragon, J. C. Estill, Y. Fu, J. A. Jeddeloh, Y. Han, H. Lee, P. Li, D. R. Lisch, S. Liu, Z. Liu, D. H. Nagel, M. C. McCann, P. SanMiguel, A. M. Myers, D. Nettleton, J. Nguyen, B. W. Penning, L. Ponnala, K. L. Schneider, D. C. Schwartz, A. Sharma, C. Soderlund, N. M. Springer, Q. Sun, H. Wang, M. Waterman, R. Westerman, T. K. Wolfgruber, L. Yang, Y. Yu, L. Zhang, S. Zhou, Q. Zhu, J. L. Bennetzen, R. K. Dawe, J. Jiang, N. Jiang, G. G. Presting, S. R. Wessler, S. Aluru, R. A. Martienssen, S. W. Clifton, W. R. McCombie, R. A. Wing, R. K. Wilson, The B73 maize genome: complexity, diversity, and dynamics. *Science* **326**, 1112–1115 (2009).

29. International Wheat Genome Sequencing Consortium (IWGSC), A chromosome-based draft sequence of the hexaploid bread wheat (*Triticum aestivum*) genome. *Science* **345**, 1251788 (2014).

30. P. R. Timilsena, E. K. Wafula, C. F. Barrett, S. Ayyampalayam, J. R. McNeal, J. D. Rentsch, M. R. McKain, K. Heyduk, A. Harkess, M. Villegente, J. G. Conran, N. Illing, B. Fogliani, C. Ané, J. C. Pires, J. I. Davis, W. B. Zomlefer, D. W. Stevenson, S. W. Graham, T. J. Givnish, J. Leebens-Mack, C. W. dePamphilis, Phylogenomic resolution of order- and family-level monocot relationships using 602 single-copy nuclear genes and 1375 BUSCO genes. *Front. Plant Sci.* **13**, 876779 (2022).

31. T. L. Elliott, D. Spalink, I. Larridon, A. R. Zuntini, M. Escudero, J. Hackel, R. L. Barrett, S. Martín-Bravo, J. I. Márquez-Corro, C. Granados Mendoza, A. C. Mashau, K. J. Romero-Soler, D. A. Zhigila, B. Gehrke, C. O. Andrino, D. M. Crayn, M. S. Vorontsova, F. Forest, W. J. Baker, K. L. Wilson, D. A. Simpson, A. M. Muasya, Global analysis of Poales diversification - parallel evolution in space and time into open and closed habitats. *New Phytol.* **242**, 727–743 (2024).

32. L. HANSON, A. BOYD, M. A. T. JOHNSON, M. D. BENNETT, First Nuclear DNA C-values for 18 Eudicot Families. *Ann. Bot.* **96**, 1315–1320 (2005).

33. P.-F. Ma, Y.-L. Liu, G.-H. Jin, J.-X. Liu, H. Wu, J. He, Z.-H. Guo, D.-Z. Li, The Pharus latifolius genome bridges the gap of early grass evolution. *Plant Cell* **33**, 846–864 (2021).

34. R. Vaser, I. Sović, N. Nagarajan, M. Šikić, Fast and accurate de novo genome assembly from long uncorrected reads. *Genome Res.* **27**, 737–746 (2017).

35. J. T. Lovell, A. Sreedasyam, M. E. Schranz, M. Wilson, J. W. Carlson, A. Harkess, D. Emms, D. M. Goodstein, J. Schmutz, GENESPACE tracks regions of interest and gene copy number variation across multiple genomes. *Elife* **11** (2022).

36. H. Tang, J. E. Bowers, X. Wang, R. Ming, M. Alam, A. H. Paterson, Synteny and Collinearity in Plant Genomes. *Science* **320**, 486–488 (2008).

37. A. H. Paterson, J. E. Bowers, R. Bruggmann, I. Dubchak, J. Grimwood, H. Gundlach, G. Haberer, U. Hellsten, T. Mitros, A. Poliakov, J. Schmutz, M. Spannagl, H. Tang, X. Wang, T. Wicker, A. K. Bharti, J. Chapman, F. A. Feltus, U. Gowik, I. V. Grigoriev, E. Lyons, C. A. Maher, M. Martis, A. Narechania, R. P. Otillar, B. W. Penning, A. A. Salamov, Y. Wang, L. Zhang, N. C. Carpita, M. Freeling, A. R. Gingle, C. T. Hash, B. Keller, P. Klein, S. Kresovich, M. C. McCann, R. Ming, D. G. Peterson, Mehboob-ur-Rahman, D. Ware, P. Westhoff, K. F. X. Mayer, J. Messing, D. S. Rokhsar, The Sorghum bicolor genome and the diversification of grasses. *Nature* **457**, 551–556 (2009).

38. Y. Jiao, J. Li, H. Tang, A. H. Paterson, Integrated Syntenic and Phylogenomic Analyses Reveal an Ancient Genome Duplication in Monocots. *Plant Cell* **26**, 2792–2802 (2014).

39. M. R. McKain, M. C. Estep, R. Pasquet, D. J. Layton, D. M. V. Díaz, J. Zhong, J. G. Hodge, S. T. Malcomber, G. Chipabika, B. Pallangyo, E. A. Kellogg, Ancestry of the two subgenomes of maize. bioRxiv [Preprint] (2018). https://doi.org/10.1101/352351.

40. S. K. Deb, P. P. Edger, J. C. Pires, M. R. McKain, Patterns, mechanisms, and consequences of homoeologous exchange in allopolyploid angiosperms: a genomic and epigenomic perspective. *New Phytol.* **238**, 2284–2304 (2023).

41. O. Jaillon, J.-M. Aury, B. Noel, A. Policriti, C. Clepet, A. Casagrande, N. Choisne, S. Aubourg, N. Vitulo, C. Jubin, A. Vezzi, F. Legeai, P. Hugueney, C. Dasilva, D. Horner, E. Mica, D. Jublot, J. Poulain, C. Bruyère, A. Billault, B. Segurens, M. Gouyvenoux, E. Ugarte, F. Cattonaro, V. Anthouard, V. Vico, C. Del Fabbro, M. Alaux, G. Di Gaspero, V. Dumas, N. Felice, S. Paillard, I. Juman, M. Moroldo, S. Scalabrin, A. Canaguier, I. Le Clainche, G. Malacrida, E. Durand, G. Pesole, V. Laucou, P. Chatelet, D. Merdinoglu, M. Delledonne, M. Pezzotti, A. Lecharny, C. Scarpelli, F. Artiguenave, M. E. Pè, G. Valle, M. Morgante, M. Caboche, A.-F. Adam-Blondon, J. Weissenbach, F. Quétier, P. Wincker, The grapevine genome sequence suggests ancestral hexaploidization in major angiosperm phyla. *Nature* **449**, 463–467 (2007).

42. J. H. Leebens-Mack, M. S. Barker, E. J. Carpenter, M. K. Deyholos, M. A. Gitzendanner, S. W. Graham, I. Grosse, Z. Li, M. Melkonian, S. Mirarab, M. Porsch, M. Quint, S. A. Rensing, D. E. Soltis, P. S. Soltis, D. W. Stevenson, K. K. Ullrich, N. J. Wickett, L. DeGironimo, P. P. Edger, I. E. Jordon-Thaden, S. Joya, T. Liu, B. Melkonian, N. W. Miles, L. Pokorny, C. Quigley, P. Thomas, J. C. Villarreal, M. M. Augustin, M. D. Barrett, R. S. Baucom, D. J. Beerling, R. M. Benstein, E. Biffin, S. F. Brockington, D. O. Burge, J. N. Burris, K. P. Burris, V. Burtet-Sarramegna, A. L. Caicedo, S. B. Cannon, Z. Çebi, Y. Chang, C. Chater, J. M. Cheeseman, T. Chen, N. D. Clarke, H. Clayton, S. Covshoff, B. J. Crandall-Stotler, H. Cross, C. W. dePamphilis, J. P. Der, R. Determann, R. C. Dickson, V. S. Di Stilio, S. Ellis, E. Fast, N. Feja, K. J. Field, D. A. Filatov, P. M. Finnegan, S. K. Floyd, B. Fogliani, N. García, G. Gâteblé, G. T. Godden, F. (Qi Y. Goh, S. Greiner, A. Harkess, J. M. Heaney, K. E. Helliwell, K. Heyduk, J. M. Hibberd, R. G. J. Hodel, P. M. Hollingsworth, M. T. J. Johnson, R. Jost, B. Joyce, M. V. Kapralov, E. Kazamia, E. A. Kellogg, M. A. Koch, M. Von Konrat, K. Könyves, T. M. Kutchan, V. Lam, A. Larsson, A. R. Leitch, R. Lentz, F.-W. Li, A. J. Lowe, M. Ludwig, P. S. Manos, E. Mavrodiev, M. K. McCormick, M. McKain, T. McLellan, J. R. McNeal, R. E. Miller, M. N. Nelson, Y. Peng, P. Ralph, D. Real, C. W. Riggins, M. Ruhsam, R. F. Sage, A. K. Sakai, M. Scascitella, E. E. Schilling, E.-M. Schlösser, H. Sederoff, S. Servick, E. B. Sessa, A. J. Shaw, S. W. Shaw, E. M. Sigel, C. Skema, A. G. Smith, A. Smithson, C. N. Stewart, J. R. Stinchcombe, P. Szövényi, J. A. Tate, H. Tiebel, D. Trapnell, M. Villegente, C.-N. Wang, S. G. Weller, M. Wenzel, S. Weststrand, J. H. Westwood, D. F. Whigham, S. Wu, A. S. Wulff, Y. Yang, D. Zhu, C. Zhuang, J. Zuidof, M. W. Chase, J. C. Pires, C. J. Rothfels, J. Yu, C. Chen, L. Chen, S. Cheng, J. Li, R. Li, X. Li, H. Lu, Y. Ou, X. Sun, X. Tan, J. Tang, Z. Tian, F. Wang, J. Wang, X. Wei, X. Xu, Z. Yan, F. Yang, X. Zhong, F. Zhou, Y. Zhu, Y. Zhang, S. Ayyampalayam, T. J. Barkman, N. Nguyen, N. Matasci, D. R. Nelson, E. Sayyari, E. K. Wafula, R. L. Walls, T. Warnow, H. An, N. Arrigo, A. E. Baniaga, S. Galuska, S. A. Jorgensen, T. I. Kidder, H. Kong, P. Lu-Irving, H. E. Marx, X. Qi, C. R. Reardon, B. L. Sutherland, G. P. Tiley, S. R. Welles, R. Yu, S. Zhan, L. Gramzow, G. Theißen, G. K.-S. Wong, One Thousand Plant Transcriptomes Initiative, One thousand plant transcriptomes and the phylogenomics of green plants. *Nature* **574**, 679–685 (2019).

43. S. C. Zeeman, J. Kossmann, A. M. Smith, Starch: Its Metabolism, Evolution, and Biotechnological Modification in Plants. *Ann. Rev. Plant Biol.* **61**, 209–234 (2010).

44. G. J. MacNeill, S. Mehrpouyan, M. A. A. Minow, J. A. Patterson, I. J. Tetlow, M. J. Emes, Starch as a source, starch as a sink: the bifunctional role of starch in carbon allocation. *J. Exp. Bot.* **68**, 4433–4453 (2017).

45. H. P. Linder, C. E. R. Lehmann, S. Archibald, C. P. Osborne, D. M. Richardson, Global grass (Poaceae) success underpinned by traits facilitating colonization, persistence and habitat transformation. *Biol. Rev. Camb. Philos. Soc.* **93**, 1125–1144 (2018).

46. B. Pfister, S. C. Zeeman, Formation of starch in plant cells. *Cell. Mol. Life Sci.* **73**, 2781–2807 (2016).

47. D. M. Beckles, A. M. Smith, T. ap Rees, A Cytosolic ADP-Glucose Pyrophosphorylase Is a Feature of Graminaceous Endosperms, But Not of Other Starch-Storing Organs1. *Plant Physiol.* **125**, 818–827 (2001).

48. B. Huang, T. A. Hennen-Bierwagen, A. M. Myers, Functions of Multiple Genes Encoding ADP-Glucose Pyrophosphorylase Subunits in Maize Endosperm, Embryo, and Leaf. *Plant Physiol.* **164**, 596–611 (2014).

49. N. J. Patron, B. Greber, B. F. Fahy, D. A. Laurie, M. L. Parker, K. Denyer, The lys5 Mutations of Barley Reveal the Nature and Importance of Plastidial ADP-Glc Transporters for Starch Synthesis in Cereal Endosperm. *Plant Physiol.* **135**, 2088–2097 (2004).

50. T. Konishi, Y. Sasaki, Compartmentalization of two forms of acetyl-CoA carboxylase in plants and the origin of their tolerance toward herbicides. *Proc. Natl. Acad. Sci. U. S. A.* **91**, 3598–3601 (1994).

51. Y. SASAKI, Y. NAGANO, Plant Acetyl-CoA Carboxylase: Structure, Biosynthesis, Regulation, and Gene Manipulation for Plant Breeding. *Biosci. Biotechnol. Biochem.* **68**, 1175–1184 (2004).

52. C. Délye, X.-Q. Zhang, S. Michel, A. Matéjicek, S. B. Powles, Molecular Bases for Sensitivity to Acetyl-Coenzyme A Carboxylase Inhibitors in Black-Grass. *Plant Physiol.* **137**, 794–806 (2005).

53. A. C. Neish, Formation of *m*- and *p*-coumaric acids by enzymatic deamination of the corresponding isomers of tyrosine. *Phytochemistry* **1**, 1–24 (1961).

54. M. Kordi, M. S. Bansal, "TreeSolve: Rapid Error-Correction of Microbial Gene Trees" in *Algorithms for Computational Biology*, C. Martín-Vide, M. A. Vega-Rodríguez, T. Wheeler, Eds. (Springer International Publishing, Cham, 2020), pp. 125–139.

55. K. T. Watts, P. C. Lee, C. Schmidt-Dannert, Biosynthesis of plant-specific stilbene polyketides in metabolically engineered Escherichia coli. *BMC biotechnol.* **6**, 22 (2006).

56. S.-Y. Jun, S. A. Sattler, G. S. Cortez, W. Vermerris, S. E. Sattler, C. Kang, Biochemical and Structural Analysis of Substrate Specificity of a Phenylalanine Ammonia-Lyase. *Plant Physiology* **176**, 1452–1468 (2018).

57. G. V. Louie, M. E. Bowman, M. C. Moffitt, T. J. Baiga, B. S. Moore, J. P. Noel, Structural Determinants and Modulation of Substrate Specificity in Phenylalanine-Tyrosine Ammonia-Lyases. *Chem. Biol.* **13**, 1327–1338 (2006).

58. Z. Yang, PAML 4: phylogenetic analysis by maximum likelihood. *Mol. Biol. Evol.* **24**, 1586–1591 (2007).

59. H. A. Maeda, Harnessing evolutionary diversification of primary metabolism for plant synthetic biology. *J. Biol. Chem.* **294**, 16549–16566 (2019).

60. Z. Bata, Z. Molnár, E. Madaras, B. Molnár, E. Sánta-Bell, A. Varga, I. Leveles, R. Qian, F. Hammerschmidt, C. Paizs, B. G. Vértessy, L. Poppe, Substrate Tunnel Engineering Aided by X-ray Crystallography and Functional Dynamics Swaps the Function of MIO-Enzymes. *ACS Catal.* **11**, 4538–4549 (2021).

61. D. Röther, L. Poppe, G. Morlock, S. Viergutz, J. Rétey, An active site homology model of phenylalanine ammonia-lyase from P. crispum. *Eur. J. Biochem.* **269**, 3065–3075 (2002).

62. F. C. Cochrane, L. B. Davin, N. G. Lewis, The Arabidopsis phenylalanine ammonia lyase gene family: kinetic characterization of the four PAL isoforms. *Phytochemistry* **65**, 1557–1564 (2004).

63. Chimpanzee Sequencing and Analysis Consortium, Initial sequence of the chimpanzee genome and comparison with the human genome. *Nature* **437**, 69–87 (2005).

64. K. Prüfer, K. Munch, I. Hellmann, K. Akagi, J. R. Miller, B. Walenz, S. Koren, G. Sutton, C. Kodira, R. Winer, J. R. Knight, J. C. Mullikin, S. J. Meader, C. P. Ponting, G. Lunter, S. Higashino, A. Hobolth, J. Dutheil, E. Karakoç, C. Alkan, S. Sajjadian, C. R. Catacchio, M. Ventura, T. Marques-Bonet, E. E. Eichler, C. André, R. Atencia, L. Mugisha, J. Junhold, N. Patterson, M. Siebauer, J. M. Good, A. Fischer, S. E. Ptak, M. Lachmann, D. E. Symer, T. Mailund, M. H. Schierup, A. M. Andrés, J. Kelso, S. Pääbo, The bonobo genome compared with the chimpanzee and human genomes. *Nature* **486**, 527–531 (2012).

65. M. E. Schranz, S. Mohammadin, P. P. Edger, Ancient whole genome duplications, novelty and diversification: the WGD Radiation Lag-Time Model. *Curr. Opin. Plant Biol.* **15**, 147–153 (2012).

66. J. C. Preston, A. Christensen, S. T. Malcomber, E. A. Kellogg, MADS-box gene expression and implications for developmental origins of the grass spikelet. *Am. J. Bot.* **96**, 1419–1429 (2009).

67. J. Barros, R. A. Dixon, Plant Phenylalanine/Tyrosine Ammonia-lyases. *Trend Plant Sci.* **25**, 66–79 (2020).

68. Y. Y. Tye, K. T. Lee, W. N. Wan Abdullah, C. P. Leh, The world availability of non-wood lignocellulosic biomass for the production of cellulosic ethanol and potential pretreatments for the enhancement of enzymatic saccharification. *Renew. Sust. Energ. Rev.* **60**, 155–172 (2016).

69. T. R. Hodkinson, Evolution and taxonomy of the grasses (Poaceae): A model family for the study of species-rich groups, *Ann. Plant Rev.* (2018)pp. 1–39.

Acknowledgements

We greatly appreciate valuable discussions with Drs. Thomas J. Givnish for the selection of monocot species, Drs. Barbara Briggs and Elizabeth Kellogg for the *Ecdeiocolea monostachya* genome sequencing and analysis, and Drs. Jaime Barros-Rios and Richard Dixon for grass PTAL functions. We thank Dr. Jorge El-Azaz for his assistance with the biochemical analysis of PALs/PTALs, Sarah Friedrich from the UW Botany Media Studio for illustration, and Cara Steekstra from the UW-Madison Botany Greenhouse for the growth of *Joinvillea ascendens.*

Funding: This work was supported by the U.S. National Science Foundation (NSF) Plant Genome Research Program (IOS-1836824) to H.A.M.. Y.T-K. was partly supported by the Oversea research fellow of the Japan Society for the Promotion of Science (JSPS). Funding for the *Ecdeiocolea monostachya* sequencing includes United Kingdom Research and Innovation-Biotechnology and Biological Sciences Research Council (BBSRC) Norwich Research Park Doctoral Training Partnership (grant no. BB/M011216/1 to S.H.) and Institute Strategic Programme (grant no. BB/P012574/1 to M.J.M. and BBS/E/J/000PR9795 to M.J.M.), Gatsby Charitable Foundation (M.J.M.), and United States Department of Agriculture-Agricultural Research Service CRIS #5062-21220-025-000D (M.J.M.). The sequencing, assembly and annotation of *Typha latifolia*, *Joinvillea ascendens*, and *Pharas latifolius* genomes was conducted by the U.S. Department of Energy Joint Genome Institute (https://ror.org/04xm1d337; proposal: 10.46936/10.25585/60001405), a DOE Office of Science User Facility, supported by the Office of Science of the U.S. Department of Energy operated under Contract No. DE-AC02-05CH11231.

Authors contributions: H.A.M., J.H.L-M, M.R.M., M.J.M., and J.S. conceptualized the research. Y.T-K., B.M., S.H., M.B., M.O., D.L., J.G., M.W., L.B.B., and K.B. performed the experiments. Y.T-K., B.M., M.R.M., S.K.D., M.J.M., S.H., J.J., C.P., S.S., K.B., D.M.G., J.S., and H.A.M. analyzed data. The original draft was written by Y.T-K., H.A.M., J.H.L-M., S.H., M.J.M. and J.J. The manuscript was reviewed and edited by Y.T-K., B.M., H.A.M., J.H.L-M., S.H., M.J.M., M.R.M., J.J. and J.S.

Competing interests: Y.T-K, B.M., and H.A.M. have a pending patent application related to the two mutations that can convert PAL enzymes into PTAL enzymes. The other authors declare that they have no competing interests related to this work.

Data and materials availability: The raw PacBio and Illumina gDNA sequencing and RNAseq data for *Ecdeiocolea monostachya* is deposited in the NCBI database under BioProject code PRJNA894727. This *Ecdeiocolea monostachya* Whole Genome Shotgun project has been deposited at DDBJ/ENA/GenBank under BioProject codes PRJNA894727 (Illumina/Oxford Nanopore Technology hybrid assembly) and PRJNA1179411 (PacBio HiFi assembly; this version used in this paper). Code not previously published for the high-throughput production of cleaned alignments for phylogenetic reconstruction is available here: https://github.com/mrmckain/Polyploid_Genomics_Utilities. The rest of genomes available in Phytozome as listed in the Resource Table (table S16). All other data reported in this paper will be shared by the lead contacts upon request.

646 ## Supplementary Materials

647 Materials and Methods
648 Figs. S1 to S11
649 Table S1 to S16
650 References (*70-109*)
651
652
653 ## Tables and Figures

654 **Table 1.** Summary statistics of the genome assembly of *J. ascendens*, *E. monostachya*, *P. latifolius,*
655 and *T. latifolia.*
656

Feature	*J. ascendens*	*E. monostachya*	*P. latifolius*	*T. latifolia*
Total length	1.21 Gb	897 Mb	1.12 Gb	215 Mb
Number of scaffolds	684	1,114	198	16
N50	63.7 Mb	1.7 Mb	97.0 Mb	14.6 Mb
Longest scaffold	89.4 Mb	12.4 Mb	115.8 Mb	24.1 Mb
Mean scaffold length	1.8 Mb	805 kb	5.6 Mb	13.5 Mb
BUSCO genes	98%	97.9%	98.4%	99.7%

657

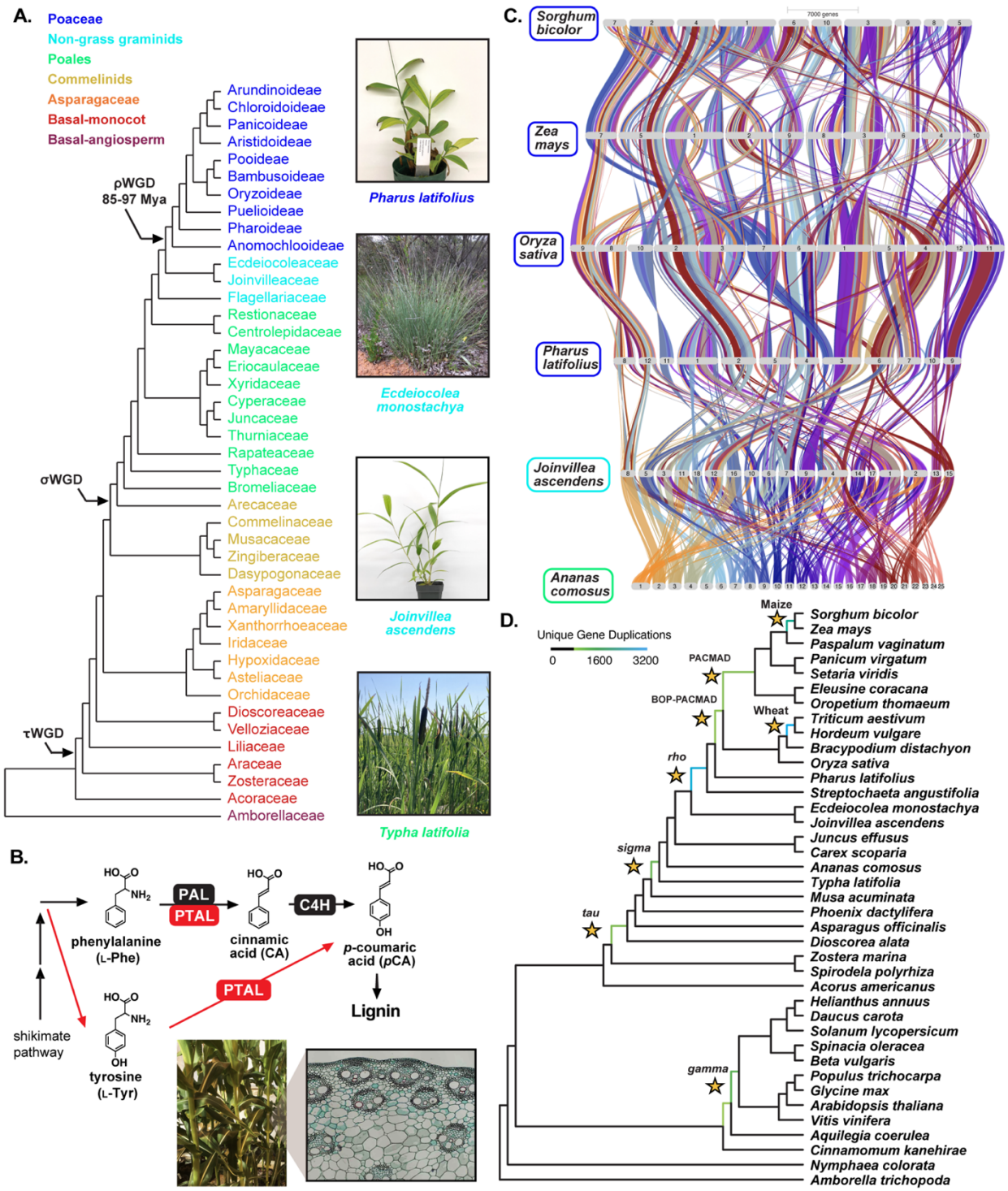

Fig. 1: Sequencing genomes of Poaceae sisters to trace the evolutionary history of grass metabolic innovations.

(A) The family tree of monocot plants showing three ancient whole genome duplication (WGD) events and the images of three plant species sister to core grasses. **(B)** Grasses have a unique metabolic trait, the dual entry pathways to synthesize lignin and phenylpropanoids from both L-phenylalanine (Phe) and L-tyrosine (Tyr) due to the presence of Phe/Tyr ammonia lyase (PTAL).

A stem cross section of *Zea mays* showing scattered vascular bundles (Image by Michael Clayton). **(C)** The whole genome comparisons of gene order (synteny) across representative Poaceae and Poales. **(D)** Mapping of gene duplications counted in gene trees using the Phylogenetic Placement of Polyploidy Using Genomes (PUG) toolkit highlights ρWGD in the last common ancestor of all grasses (Poaceae), as well as sigma (σ) and tau (τ) WGDs.

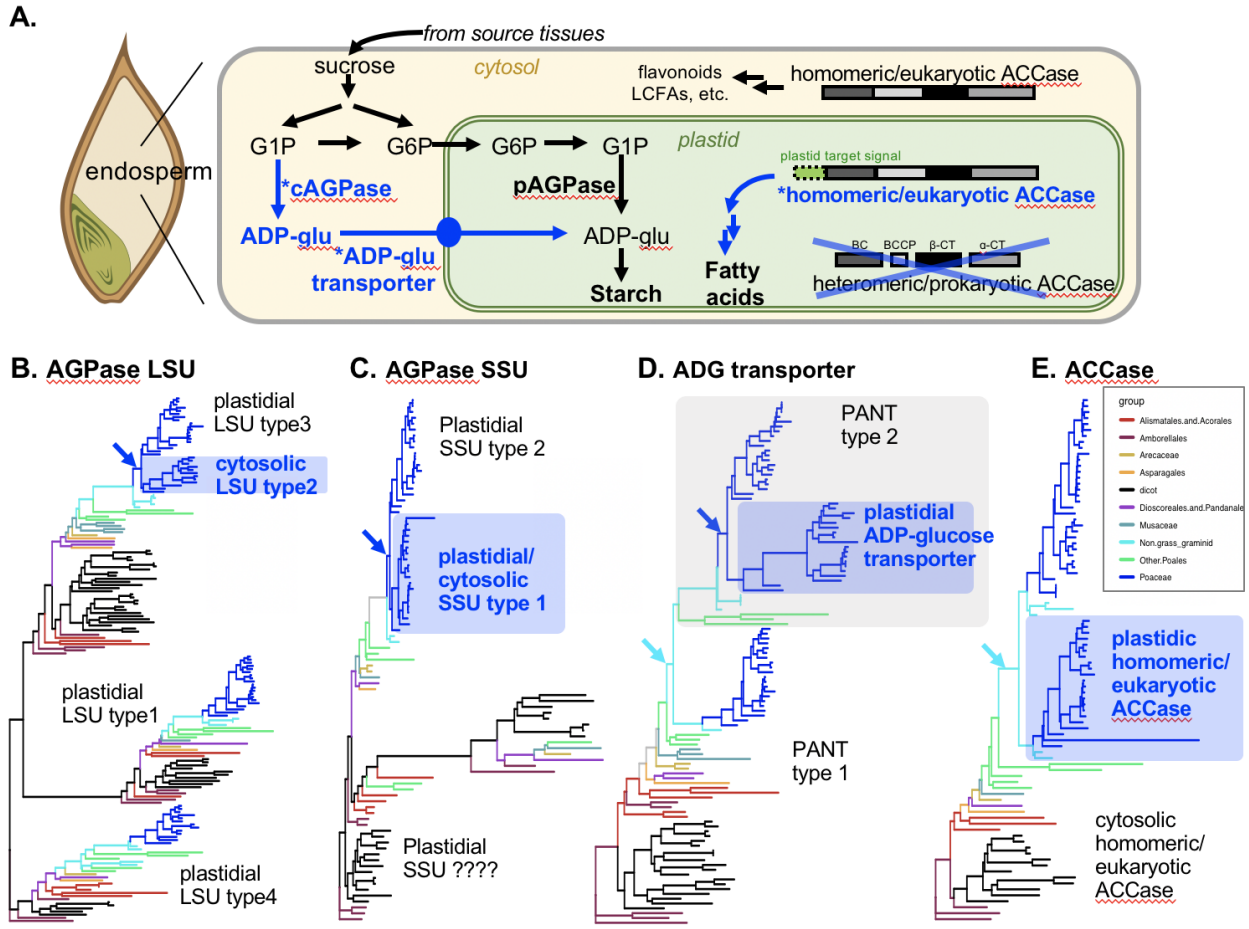

Fig. 2. Alteration of starch and fatty acid biosynthesis during the grass evolution.

(A) In the endosperm of grasses, starch can be synthesized in both cytosol and plastids due to the presence of cytosolic ADP-glucose pyrophosphorylase (AGPase) and ADP-glucose (ADG) transporter. Grasses also have unique fatty acid biosynthetic enzymes, homomeric eukaryotic-type acetyl-CoA carboxylase (ACCase) in the plastids, instead of heteromeric prokaryotic-type ACCase typically found in other plant plastids. **(B to E)** The phylogenetic trees of AGPase large subunit (LSU, **B**), small subunit (SSU, **C**), ADG transporter **(D)**, and ACCase **(E)** of grasses, Poales, as well as other monocots and angiosperms. Blue and gray boxes denote clades specific to Poaceae and non-grass graminids that likely contributed to the evolution of their unique starch and fatty acid biosynthetic pathways. Blue and sky-blue arrows indicate the underlying duplication events that occurred after and before the emergence of grasses, respectively. The original trees with branch supports and labels are shown in **fig. S1**.

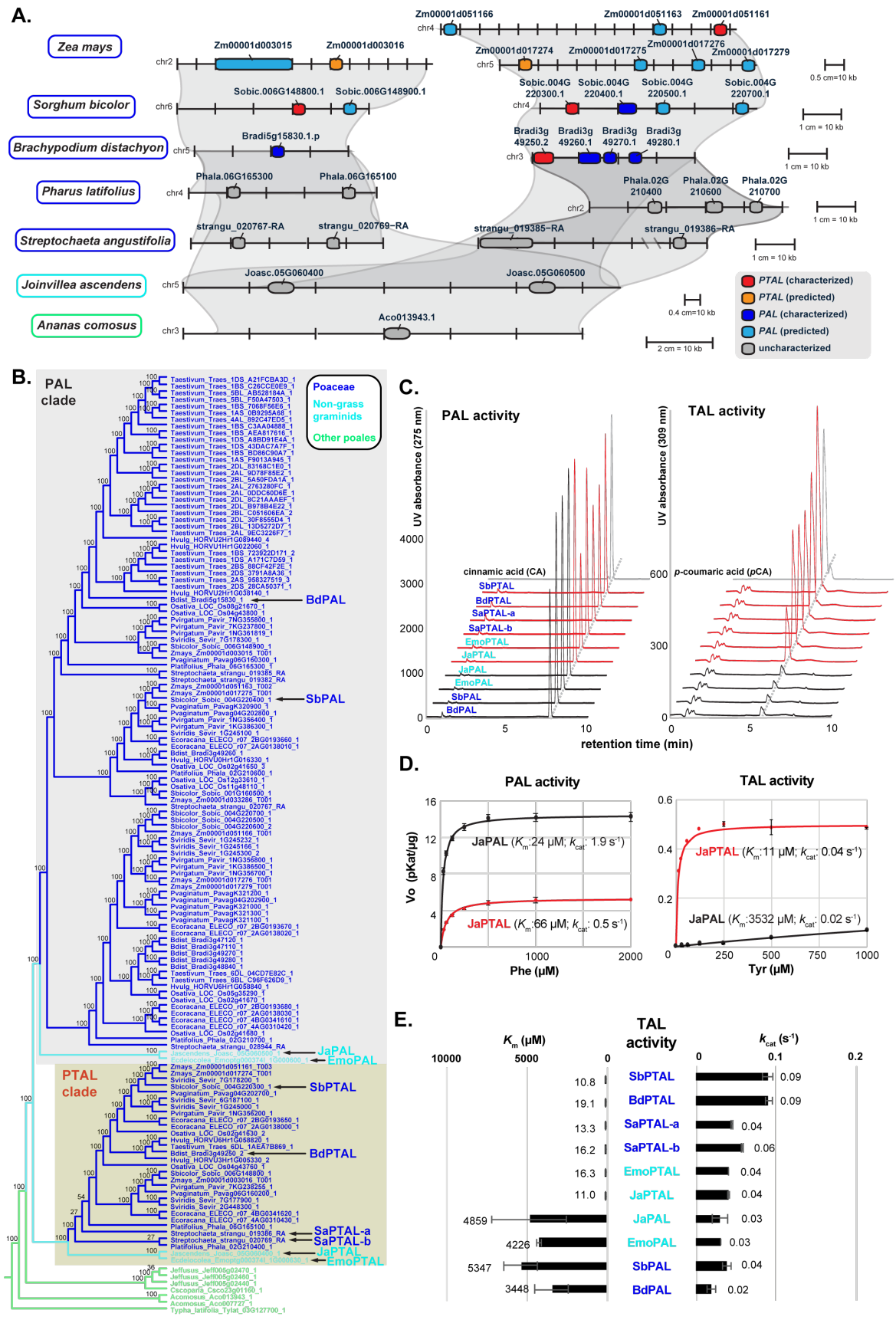
A.
Zea mays
Sorghum bicolor
Brachypodium distachyon
Pharus latifolius
Streptochaeta angustifolia
Joinvillea ascendens
Ananas comosus
Zm00001d051166
Zm00001d051163
Zm00001d051161
Zm00001d003015
Zm00001d003016
Zm00001d017274
Zm00001d017275
Zm00001d017276
Zm00001d017279
Sobic.006G148800.1
Sobic.006G148900.1
Sobic.004G 220300.1
Sobic.004G 220400.1
Sobic.004G 220500.1
Sobic.004G 220700.1
Bradi5g15830.1.p
Bradi3g 49250.2
Bradi3g 49260.1
Bradi3g 49270.1
Bradi3g 49280.1
Phala.06G165300
Phala.06G165100
Phala.02G 210400
Phala.02G 210600
Phala.02G 210700
strangu_020767-RA
strangu_020769-RA
strangu_019385-RA
strangu_019386-RA
Joasc.05G060400
Joasc.05G060500
Aco013943.1
0.5 cm=10 kb
1 cm = 10 kb
0.4 cm=10 kb
2 cm = 10 kb
PTAL (characterized)
PTAL (predicted)
PAL (characterized)
PAL (predicted)
uncharacterized
B.
PAL clade
PTAL clade
Poaceae
Non-grass graminids
Other poales
BdPAL
SbPAL
JaPAL
EmoPAL
SbPTAL
BdPTAL
SaPTAL-a
SaPTAL-b
JaPTAL
EmoPTAL
C.
PAL activity
TAL activity
UV absorbance (275 nm)
UV absorbance (309 nm)
cinnamic acid (CA)
p-coumaric acid (pCA)
SbPTAL
BdPTAL
SaPTAL-a
SaPTAL-b
EmoPTAL
JaPTAL
JaPAL
EmoPAL
SbPAL
BdPAL
retention time (min)
D.
PAL activity
TAL activity
Vo (pKat/µg)
JaPAL (Km:24 µM; kcat: 1.9 s-1)
JaPTAL (Km:66 µM; kcat: 0.5 s-1)
JaPTAL (Km:11 µM; kcat: 0.04 s-1)
JaPAL (Km:3532 µM; kcat: 0.02 s-1)
Phe (µM)
Tyr (µM)
E.
TAL activity
Km (µM)
kcat (s-1)
SbPTAL 10.8 0.09
BdPTAL 19.1 0.09
SaPTAL-a 13.3 0.04
SaPTAL-b 16.2 0.06
EmoPTAL 16.3 0.04
JaPTAL 11.0 0.04
JaPAL 4859 0.03
EmoPAL 4226 0.03
SbPAL 5347 0.04
BdPAL 3448 0.02

686

687 **Fig. 3: The PTAL enzyme evolved before the emergence of grasses through tandem**
688 **duplication predating ρWGD.**

689 **(A)** *PAL/PTAL* gene synteny is shown for *A. comosus, J. ascendens, S. angustifolia, P. latifolius,*
690 *B. distachyon, S. bicolor,* and *Z. mays*, illustrating the gains and losses of PAL/PTAL synteny
691 across Poales. The *PAL* gene is duplicated and neofunctionalized to PTAL in the ancestor of *J.*
692 *ascendens*. The *PAL*/*PTAL* pair is then duplicated within grasses, likely due to the ρWGD, and
693 again in *Z. mays*, likely due to the *Z. mays* WGD. **(B)** Phylogenetic tree of *PAL*/*PTAL* genes, with
694 focus on Poales species, generated with RAxML-NG and reconciled with TreeSolve. *PAL*/*PTAL*
695 homologs characterized in this study are highlighted with black arrows. The full-scaled
696 phylogenetic tree is shown in **fig. S5**. **(C)** HPLC trace of PAL and TAL activity assay for
697 PTALs/PALs from *S. bicolor* (SbPTAL and SbPAL), *B. distachion* (BdPTAL and BdPAL), *S.*
698 *angustifolia* (SaPTAL-a and SaPTAL-b), *J. ascendens* (JaPTAL and JaPAL) and *Ecdeiocolea*
699 *monostachya* (EmoPTAL and EmoPAL). See **fig. S6** for additional traces of their control reactions.
700 **(D)** Michaelis-Menten curves of TAL and PAL assay for JaPTAL and JaPAL. **(E)** Kinetic
701 parameters of TAL activity for PTALs/PALs. Data are means ± SD (n = 3).
702

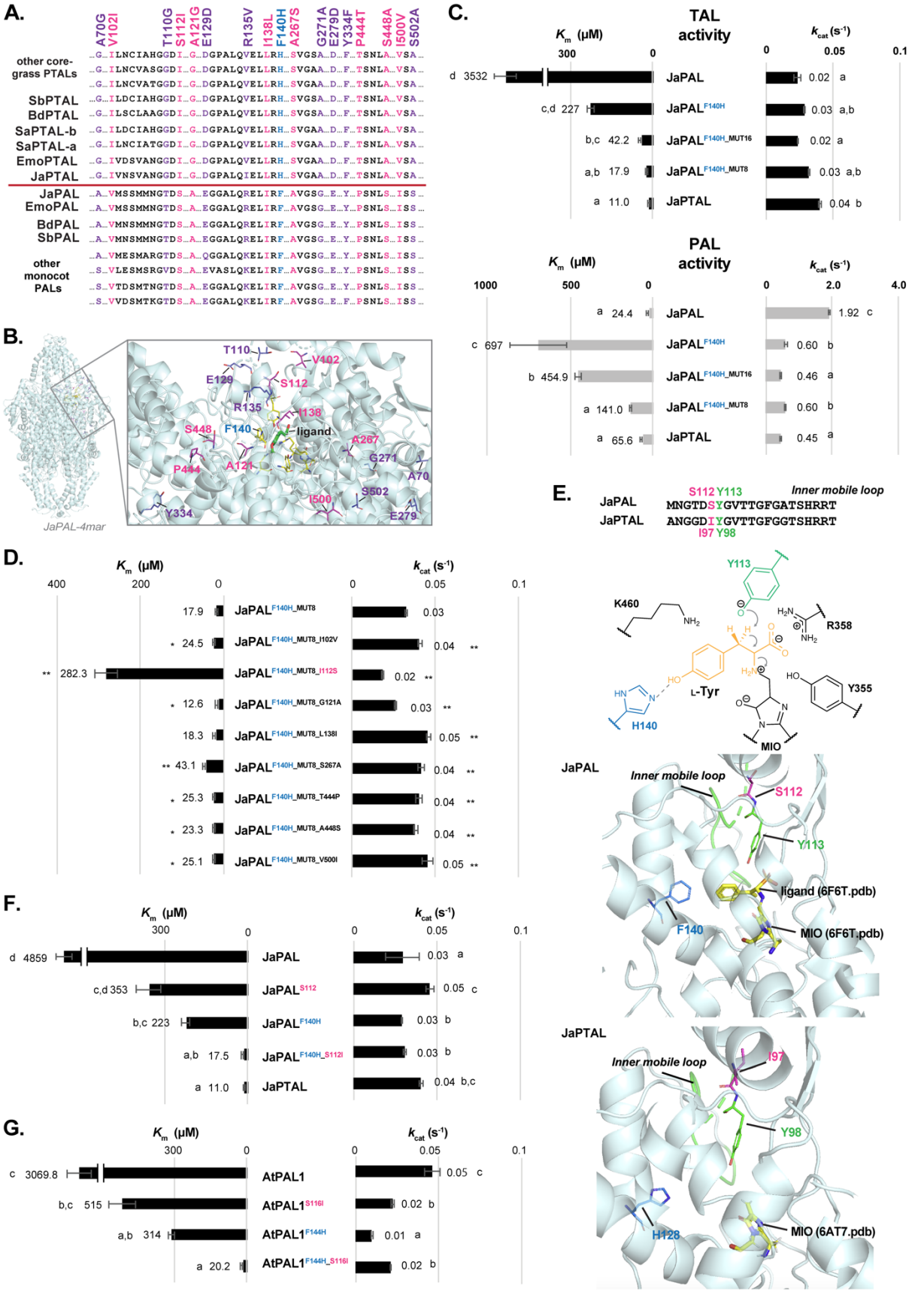
A.
A70G V102I T110G S112I A121G E129D R135V I138L F140H A267S G271A E279D Y334F P444T S448A I500V S502A
other core-grass PTALs
SbPTAL
BdPTAL
SaPTAL-b
SaPTAL-a
EmoPTAL
JaPTAL
JaPAL
EmoPAL
BdPAL
SbPAL
other monocot PALs
B.
JaPAL-4mar
T110
V402
E129
S112
R135
I138
S448
F140
ligand
A267
G271
P444
A121
A70
S502
I500
Y334
E279
C.
TAL activity
Km (μM)
kcat (s-1)
JaPAL
JaPAL F140H
JaPAL F140H_MUT16
JaPAL F140H_MUT8
JaPTAL
PAL activity
D.
JaPAL F140H_MUT8
JaPAL F140H_MUT8_I102V
JaPAL F140H_MUT8_I112S
JaPAL F140H_MUT8_G121A
JaPAL F140H_MUT8_L138I
JaPAL F140H_MUT8_S267A
JaPAL F140H_MUT8_T444P
JaPAL F140H_MUT8_A448S
JaPAL F140H_MUT8_V500I
E.
JaPAL MNGTDSYGVTTGFGATSHRRT
JaPTAL ANGGDIYGVTTGFGGTSHRRT
S112 Y113
I97 Y98
Inner mobile loop
K460
R358
Y113
L-Tyr
Y355
H140
MIO
JaPAL
Inner mobile loop
S112
Y113
ligand (6F6T.pdb)
F140
MIO (6F6T.pdb)
JaPTAL
Inner mobile loop
I97
Y98
H128
MIO (6AT7.pdb)
F.
JaPAL
JaPAL S112
JaPAL F140H
JaPAL F140H_S112I
JaPTAL
G.
AtPAL1
AtPAL1 S116I
AtPAL1 F144H
AtPAL1 F144H_S116I

703

704 **Fig. 4: Two mutations, F140H and S112I, convert PAL into PTAL enzymes.**

705 **(A)** Partial amino acid alignment highlighting residue His/Phe140 (cyan), which is essential for
706 recognizing substrate phenylalanine and tyrosine, and residues highly conserved uniquely in
707 PTALs (magenta: conserved in both PALs and PTALs, but in distinct ways; purple: conserved
708 among PTALs but not PALs). Full-scaled alignment is shown in **fig. S8**. **(B)** Protein structure
709 model of JaPAL highlighting selected residues. The structures of the substrate ligand and MIO
710 cofactor are derived from the template 6F6T.pdb. Residues important for enzyme activity are
711 displayed in yellow. **(C)** Kinetic parameters of TAL and PAL activity for JaPAL, JaPAL with
712 mutation at His140 site ($JaPAL^{F140H}$) and additional mutations ($JaPAL^{F140H_MUT8}$ and
713 $JaPAL^{F140H_MUT16}$), and JaPTAL. **(D)** Kinetic parameters of TAL activity for $JaPAL^{F140H_MUT8}$ with
714 mutation on 8 of each residue back to PAL type. **(E)** Potential mechanism of TAL reaction (*77*)
715 and roles of His140 and Ile112 for the catalysis of the PTAL enzyme. **(F)** Kinetic parameters of
716 TAL activity for JaPAL with site-directed mutation at His140 site ($JaPAL^{F140H}$) and Ile112 site
717 ($JaPAL^{S112I}$). **(G)** Kinetic parameters of TAL activity for Arabidopsis AtPAL1 with mutation at
718 His140 ($AtPAL1^{F144H}$) and Ile112 ($AtPAL1^{S116I}$). Data are means ± SD (n = 3). Different letters
719 indicate significant differences ($p < 0.05$).

720